Since January 2020 Elsevier has created a COVID-19 resource centre with free information in English and Mandarin on the novel coronavirus COVID-19. The COVID-19 resource centre is hosted on Elsevier Connect, the company's public news and information website.

Biochemical and Biophysical Research Communications 571 (2021) 152–158

Contents lists available at ScienceDirect

Biochemical and Biophysical Research Communications

journal homepage: www.elsevier.com/locate/ybbrc

A non-RBM targeted RBD specific antibody neutralizes SARS-CoV-2 inducing S1 shedding

Yingyi Long [a, b, 1], Shuyi Song [a, b, 1], Feiyang Luo [a, b], Xiaojian Han [a, b], Chao Hu [a, b], Yingming Wang [a, b], Shenglong Li [a, b], Wang Wang [a, b], Huajun Zhang [c], Bo Zhang [c], Tingting Li [a, b, **], Aishun Jin [a, b, *]

[a] Department of Immunology, College of Basic Medicine, Chongqing Medical University, Chongqing, 400010, China
[b] Chongqing Key Laboratory of Basic and Translational Research of Tumor Immunology, Chongqing Medical University, Chongqing, 400010, China
[c] State Key Laboratory of Virology, Wuhan Institute of Virology, Center for Biosafety Mega-Science, Chinese Academy of Sciences, Wuhan, 430071, China

ARTICLE INFO

Article history:
Received 9 June 2021
Received in revised form
5 July 2021
Accepted 18 July 2021
Available online 20 July 2021

Keywords:
COVID-19
SARS-CoV-2
Receptor binding motif
Neutralizing antibody
S1 shedding
Syncytia

ABSTRACT

Potent neutralizing antibodies (Abs) have been proven with therapeutic efficacy for the intervention against SARS-CoV-2. Majority of these Abs function by directly interfering with the virus entry to host cells. Here, we identified a receptor binding domain (RBD) specific monoclonal Ab (mAb) 82A6 with efficient neutralizing potency against authentic SARS-CoV-2 virus. As most Abs targeting the non-receptor binding motif (RBM) region, 82A6 was incapable to block the RBD-ACE2 interaction. In particular, it actively promoted the S1 subunit shedding from the S protein, which may lead to effective reduction of intact SARS-CoV-2 viruses. Importantly, it could block potential syncytia formation associated with post-infectious cell surface expression of S proteins. Our study evidenced a RBD specific Ab with unique beneficial efficacy against SARS-CoV-2 infection, which might bring informative significance to understand the collective effects of neutralizing Abs elicited in COVID-19 patients.

1. Introduction

Neutralizing Abs with protective effects could be elicited during SARS-CoV-2 infection or after vaccination against this virus [1–5]. SARS-CoV-2 enters the host cells through the interaction between the viral spike (S) protein, specifically the RBM region, and the host receptor angiotensin-converting enzyme 2 (ACE2) [6–9]. Consequently, the RBM has been the main target for the prophylaxis and the treatment of COVID-19 [10–14]. For Abs targeting the non RBM region [15–17], recent studies have reported that many of them also exhibit neutralizing capabilities against SARS-CoV-2, through the corresponding mechanisms were relatively less understood.

Compelling evidences have shed light on additional key steps during SARS-CoV-2 infection other than RBD-ACE2 recognition as potential targets of neutralization [10,18–20]. Naturally, subsequent to the receptor binding, the S1 subunit will dissociate from the trimeric S protein, which exposes the other subunit S2 [8,21,22]. S2, in turn, mediates the membrane fusion of the virus and the host cell, as the final step of viral entry [8,21,22]. Infected cells express the S protein on the cell surface, and can form syncytia when fused with the adjacent ACE2-expressing cell. The presence of multinucleated syncytial pneumocytes has usually been associated with severe cases of COVID-19 [23–26]. Therefore, neutralizing Abs targeting these critical processes during SARS-CoV-2 infection, including the S1 shedding and/or the formation of syncytia, may exhibit functional significance in addition to the neutralization mediated by direct blockage of receptor binding.

Here, we presented a RBD specific mAb 82A6 targeting the non-RBM region, which exhibited neutralizing potency against authentic SARS-CoV-2 virus. This mAb did not affect the interaction between RBD and ACE2. Instead, it induced S1 shedding and blocked syncytia formation. This study provides the neutralizing mechanism for a non-RBM targeted mAb with unique beneficial efficacy against SARS-CoV-2, and enriches our understanding of the relationship between S1 shedding and syncytia formation.

* Corresponding author. Department of Immunology, College of Basic Medicine, Chongqing Medical University, Chongqing, 400010, China.
** Corresponding author. Department of Immunology, College of Basic Medicine, Chongqing Medical University, Chongqing, 400010, China.
E-mail addresses: tingtingli1191@cqmu.edu.cn (T. Li), aishunjin@cqmu.edu.cn (A. Jin).
[1] The two co-first authors contributed equally to this work.

https://doi.org/10.1016/j.bbrc.2021.07.062
0006-291X/

2. Materials and methods

2.1. Recombinant antibody production and purification

Recombinant antibody was produced and purified based on our published method [4].

2.2. Surface plasmon resonance (SPR) experiment

The affinity between the mAb and SARS-CoV-2 RBD was measured by SPR. The anti-human Fc antibody was immobilized on the CM5 chip (GE Healthcare, USA) to capture antibodies. After the binding of detected mAb by the chip, the gradient concentrations of SARS-CoV-2 RBD were flowed through the sensor chip system. The affinity of mAb was calculated by 1:1 binding model with Biacore X100 evaluation software (version 2.0.2).

In order to determine the inhibition rate of mAbs on the ACE-RBD interaction, SARS-CoV-2 RBD was loaded on CM5 sensor chip about to 250 RUs. Then ACE2 (20 μg/mL) was injected for 60 s in the present or absence of the mAbs. The blocking efficacy was determined by comparing the response units with and without prior antibody incubation.

2.3. Peptide ELISA

Peptide ELISA was performed based on our published method [27].

2.4. Competitive ELISA

For the competitive ELISA, 384-well plates were coated with 2 μg/mL recombinant RBD-his (Sino Biological, Beijing, China) at 4 °C overnight. The serially diluted antibodies were added to the plates for the incubation at 37 °C for 40 min. Next, 200 ng/mL ACE2-mFc (Sino Biological, Beijing, China) was added at 37 °C for 40 min. Then, the plates were incubated with ALP-conjugated anti-human IgG antibody (Thermo Fisher (Waltham, MA, USA), cat. no. a18808, 1:2000) at 37 °C for 30 min. For the quantification of bound IgG, PNPP (Thermo Fisher) was added and the absorbance at 405 nm was measured by the MultiSkan GO fluoro-microplate reader (Thermo Fisher).

2.5. Pseudotyped virus packaging and neutralizing

The packaging plasmid bearing SARS-CoV-2 S protein was constructed and co-transfected into 293T cells with pWPXL-lenti-Luciferase-EGFP, pSPAX2. After 48 h post-transfection, the supernatants containing pseudovirus were harvested and filtered through the 0.45 μm filter. To determine the neutralizing potency of mAbs, the pseudovirus were incubated with an equal volume (50 μL) of serially diluted mAbs at 37 °C for 1 h. Then the antibody-pseudovirus mixture was added to cell seeded plate. After cultured at 37 °C for 72 h, luciferase activities were detected by the Bright-Luciferase Reporter Assay System (Promega (Wisconsin, USA), cat. no. E2650). The IC_{50} values were determined using 4-parameter logistic regression (GraphPad Prism version 8).

2.6. Authentic SARS-CoV-2 neutralization assay

The neutralizing of 82A6 against authentic SARS-CoV-2 virus was performed via PRNT in a biosafety level 3 laboratory of Wuhan Institute of Virology based on our published method [27].

2.7. Flow cytometry receptor binding inhibition assay

The mAbs (final concentration of 100 μg/mL) were incubated with 10 μg/mL recombinant RBD-his (Sino Biological, Beijing, China) at 37 °C for 1 h. Then the mixture was incubated with 5×10^5 293T cells expressing ACE2 (293T/ACE2) at room temperature (RT) for 30 min. After washing twice, the cells stained with anti-his tag antibody conjugated with PE (BioLegend (California, USA), cat. no. 362603) and anti-human IgG antibody APC (BioLegend (California, USA), cat. no. 409306) at RT for 30 min. After resuspending, the labeled cells were detected by flow cytometry (BD Celesta). The data in FCS format were analyzed by FlowJo X.

2.8. The detection of S1 shedding via flow cytometry

The pcDNA3.4 vector (pcDNA3.4-SARS-CoV-2-S) containing full-length SARS-CoV-2 S protein was transiently transfected into 293T cells. The detection of S1 shedding induced by 82A6 with different incubation time was refer to the method of Zhang [10]. Briefly, the 293T/ACE2 cells were used to capture the S1 subunit released into the supernatant of the 82A6 and 293T/S cells co-culture system. After washing twice, samples were stained with anti-Human IgG conjugated with PerCP/Cy5.5 (BioLegend (California, USA), cat. no. 410710) at RT for 30 min and the samples were treated and detected as the above-mentioned.

2.9. Western blot analysis of S1 in the cell supernatant

293T cells carrying surface expression of SARS-CoV-2 S protein (293T/S) were incubated with 10 μg testing mAbs at 37 °C for 1 h. The obtained supernatants were collected by centrifugation and mixed with 5 × SDS-PAGE loading buffer (Beyotime, Shanghai, China). After the denaturation, samples were subjected to electrophoresis with 7.5% SDS-polyacrylamide gel and then transferred to polyvinylidene fluoride membrane (PVDF). The *anti*-SARS-CoV-2 Spike S1 Antibody and HRP-conjugated mouse anti-human secondary antibody (Abcam, ab99757, 1:10000) were used as primary and secondary antibody respectively. The membrane was detected by Bio-rad ChemiDoc imaging system (Bio-rad).

2.10. Cell–cell fusion assay

The pcDNA3.4-SARS-CoV-2 S and pWPXL-EGFP were co-transfected into 293T cells. After 48 h of transfection, the cells were digested with trypsin (0.25%) and incubated with the mAbs at 37 °C for 1 h. Then the cells were added to 293T/ACE2 cells. After incubating at 37 °C for 3 h, the multinuclear syncytia were observed and photographed by fluorescence microscope. The nuclei number of syncytia was counted by Image J.

2.11. Data analysis

Data are shown as mean ± SEM. Student's t-test was used to compare the two groups. The difference was considered significant if $p < 0.05$.

3. Results

3.1. 82A6 neutralized authentic SARS-CoV-2 virus

The mAb 82A6 was obtained from the memory B cells of COVID-19 convalescent patients [4]. We first confirmed that 82A6 could bind to SARS-CoV-2 RBD by ELISA, with the half efficient concentration (EC_{50}) of 0.007 μg/mL (Fig. 1A). Also, 82A6 showed a high binding potency to RBD, with an affinity constant (K_D) of 2 nM, as

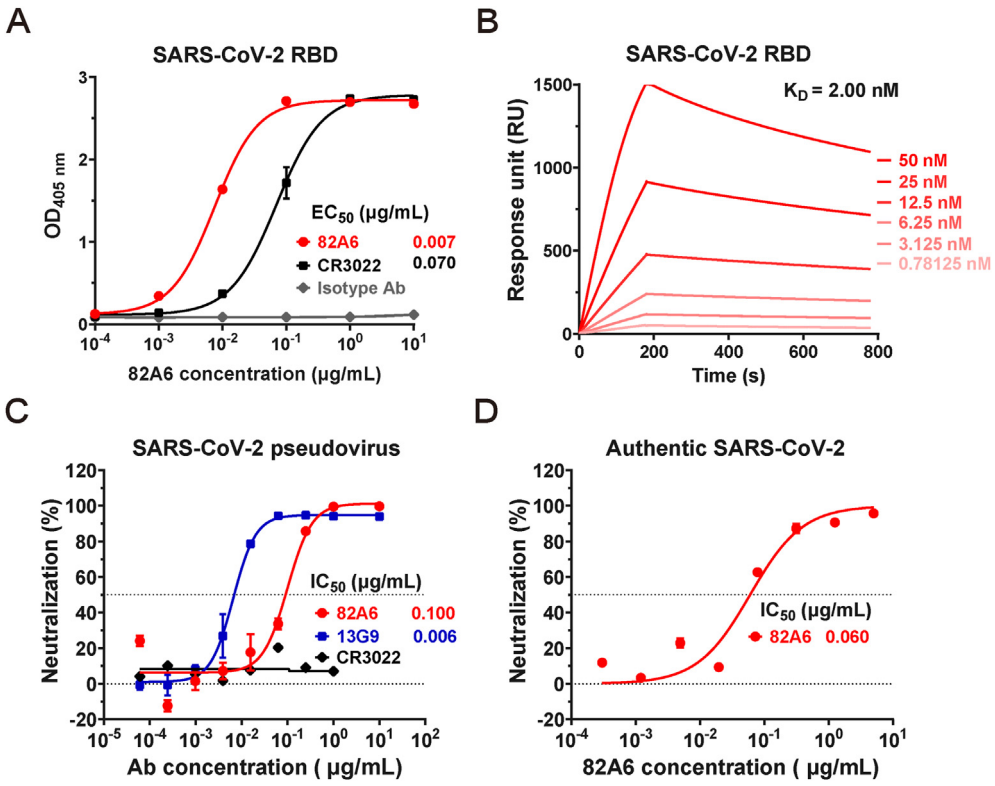

Fig. 1. The binding affinity and the neutralizing efficacy of 82A6. (A) ELISA was used to study the binding ability of the mAbs 82A6, CR3022 and isotype Ab to the recombinant SARS-CoV-2 RBD, with serial dilutions. (B) The binding kinetics of 82A6 to RBD was measured by SPR. (C) The neutralizing potency of 82A6 against pseudovirus bearing SARS-CoV-2 S protein was measured by pseudovirus neutralization assay. RBM specific neutralizing mAb 13G9 was used as the positive control. (D) The neutralizing potency of 82A6 against authentic SARS-CoV-2 virus. Dashed line indicated 0% or 50% reduction in the viral infectivity. Data were obtained from a representative experiment of at least two replicates, presented as mean ± SEM.

identified by the surface plasmon resonance (SPR) assay (Fig. 1B). Moreover, we assessed the neutralizing capability of 82A6 against the pseudovirus bearing SARS-CoV-2 S protein and authentic SARS-CoV-2 virus. We found that 82A6 efficiently blocked the pseudovirus, with the half inhibition concentration (IC_{50}) of 0.100 μg/mL (Fig. 1C). The plaque reduction neutralization test revealed that 82A6 could also effectively neutralize the authentic virus, with the IC_{50} of 0.060 μg/mL (Fig. 1D). These data demonstrated that 82A6 was a RBD specific mAb that was capable of neutralizing authentic SARS-CoV-2 virus.

3.2. A non-RBM region $S^{334-353}$ contributed to the antigenic site recognized by 82A6

Next, we tested whether 82A6 targeted the RBM region, as the majority of RBD specific neutralizing Abs. For this purpose, a previously identified RBM specific mAb 13G9 showing complete blockage of the ACE2 binding was chosen as positive control. Unlike 13G9, 82A6 was not capable of interrupting the interaction between RBD and ACE2, as shown by competitive ELISA (Fig. 2A). In parallel, the SPR assay demonstrated that the pre-binding of 82A6 to RBD did not affect the subsequent interaction of ACE2 with RBD (Fig. 2B). This phenomenon was further confirmed using 293T cells expressing ACE2. We found that RBD could simultaneously bind to 82A6 and the ACE2 protein, which was not observed for the RBM specific 13G9 (Fig. 2C). These results indicated that the neutralizing Ab 82A6 might target a non-RBM region within RBD, likely associated with a mechanism other than affecting the recognition of RBD to ACE2.

To investigate the antigenic site recognized by 82A6, we screened for any potential linear sites that could be targeted by 82A6, via Western blot analysis against the denatured RBD. In fact, a direct interaction between 82A6 and the linear structure of SARS-CoV-2 RBD was detected (Fig. 2D). To address such recognition in detail, we designed and synthesized a series of 20-mer peptides (RBD1 to RBD15) overlapped with 5 amino acids to cover the entire RBD, corresponding to the amino acids 319–541 of SARS-CoV-2 S ($S^{319-541}$) [27]. As shown by the peptide ELISA, 82A6 could bind to two distinct peptides RBD2 ($S^{334-353}$) and RBD13 ($S^{499-518}$) (Fig. 2E). RBD modeling revealed that the majority of the amino acid residues of RBD2 ($S^{334-353}$) were located on the surface of the natural structure of RBD, indicating a high probability of this region taking part in the steric antigenic site of 82A6 (Fig. 2G). On the contrary, majority of the 20 residues within RBD13 ($S^{499-518}$) were identified to be buried within the native RBD structure, challenging its contribution to 82A6 steric epitope (Fig. 2G). To determine which amino acids within RBD13 ($S^{499-518}$) might participate in the binding of 82A6, we individually replaced each residue of this peptide with alanine (A). Six of the twenty-point mutations rendered RBD13 unrecognizable by 82A6, shown by the significantly reduced binding ability of this mAb (Fig. 2F). However, structure reconstitution identified that all of these 6 amino acids were distributed in the inner area of RBD, thus excluding the involvement of this linear region ($S^{499-518}$) in the steric epitope for 82A6 (Fig. 2G). Collectively, we confirmed that a non-RBM region $S^{334-353}$ contributed, at least partially, to the antigenic site recognized by 82A6.

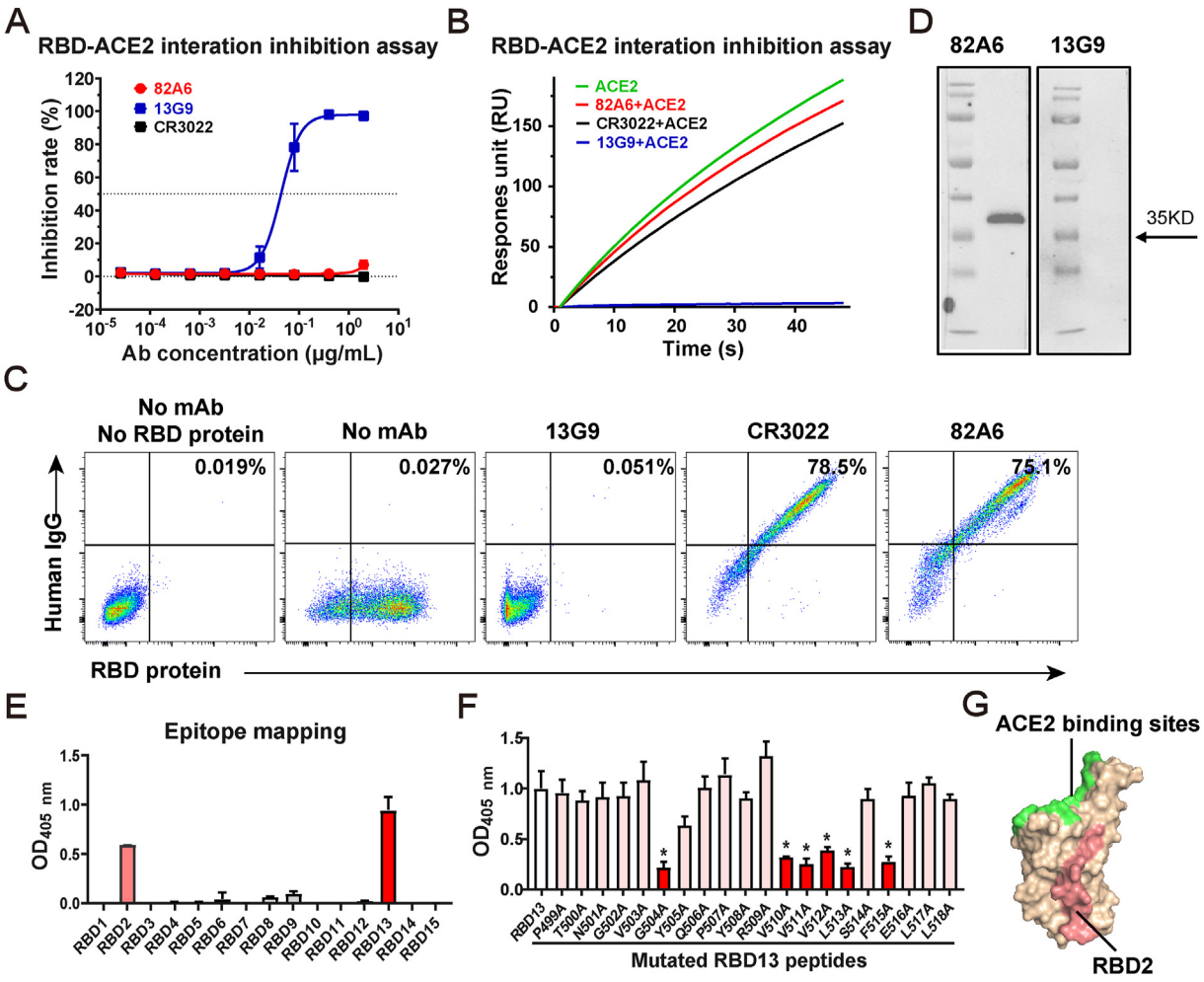

Fig. 2. 82A6 recognized a linear antigenic site on the non-RBM region within RBD. (A) The inhibition rate of 82A6 in blocking the RBD-ACE2 interaction was detected by competitive ELISA. (B) The competition of 82A6 and ACE2 for binding to SARS-CoV-2 RBD was measured by SPR. Immobilized SARS-CoV-2 RBD was saturated with the mAb (red), or without antibody (green), prior to an injection with the soluble ACE2. CR3022 (black) and 13G9 (blue) were used as negative and positive controls, respectively. (C) The binding of the RBD protein to ACE2 expressed on 293T/ACE2 cells in the presence or absence of the mAbs was tested by flow cytometry analysis. Data were obtained from a representative experiment of three replicates. (D) The binding ability of 82A6 to the denatured RBD was detected by Western blot analysis. 13G9, which is an antibody that has been shown to not bind to denatured RBD [27]. (E) The binding ability of 82A6 to the linear peptides was analyzed by peptide ELISA (n = 3). (F) ELISA results of the binding activity of 82A6 to the wild type RBD13 or peptides carrying single mutations derived from the full length RDB13 (n = 3, $*p < 0.05$). (G) The distributions of the ACE2 binding site (green) and the proposed antigenic site of 82A6 (red) on RBD. (For interpretation of the references to colour in this figure legend, the reader is referred to the Web version of this article.)

3.3. 82A6 efficiently triggered S1 shedding

To understand the potential mechanism for this non-RBM neutralizing mAb, we tested whether 82A6 could induce S1 shedding, which was another key target reported for the RBD specific Abs. To this end, 293T cells with surface expression of the S protein (293T/S) were utilized to determine S1 dissociation. Flow cytometry analysis showed that 82A6 could promote the S1 subunit to be released from 293T/S cells, relative to the negative control using a neutralizing Ab CR3022 with cross-reactivity to SARS-CoV and SARS-CoV-2 (Fig. 3A). Such 82A6-induced S1 shedding could be observed from as quickly as 5 min to 4 h, in a time-dependent manner (Fig. 3A). Alternatively, we utilized the 293T/ACE2 cells to capture the S1 subunits released into the supernatant of the 82A6 and 293T/S cell co-culture system. We found that the amounts of the free S1 were dose-dependently correlated with 82A6 concentrations (Fig. 3B). In addition, Western blot analysis confirmed that the S1 protein could only be detected in the 293T/S cell supernatant when 82A6 was added (Fig. 3C). These results indicated that 82A6 likely neutralized SARS-CoV-2 by reducing the number of intact viruses though promoting S1 shedding.

3.4. 82A6 blocked the syncytia formation

As S1 shedding has been correlated with the occurrence of SARS-CoV-2 mediated cell fusion [26], we assessed whether the neutralization by 82A6 would result in the undesired syncytia formation. EGFP-labeled 293T/S cells were co-cultured with 293T/ACE2 cells, in the presence of 82A6 or CR3022. As shown in Fig. 4A, EGFP-293T/S cells were universally single nucleic cells under the fluorescent microscope. However, when they were co-cultured with 293T/ACE2 cells, a marked increase of syncytia formation was observed (Fig. 4B). Importantly, 82A6, but not CR3022, could inhibit such cell fusion with high efficiency, shown by the significantly decreased number of multi-nucleic cells in the 82A6 co-culture system (Fig. 4A and B). These results provided direct evidence of a neutralizing Ab capable to induce S1 shedding that could, in fact, prohibit the undesired cell fusion in vitro. In summary, we identified a non-RBM targeted mAb 82A6 that neutralized SARS-CoV-2 by promoting S1 shedding, with effective blockage of the syncytia formation.

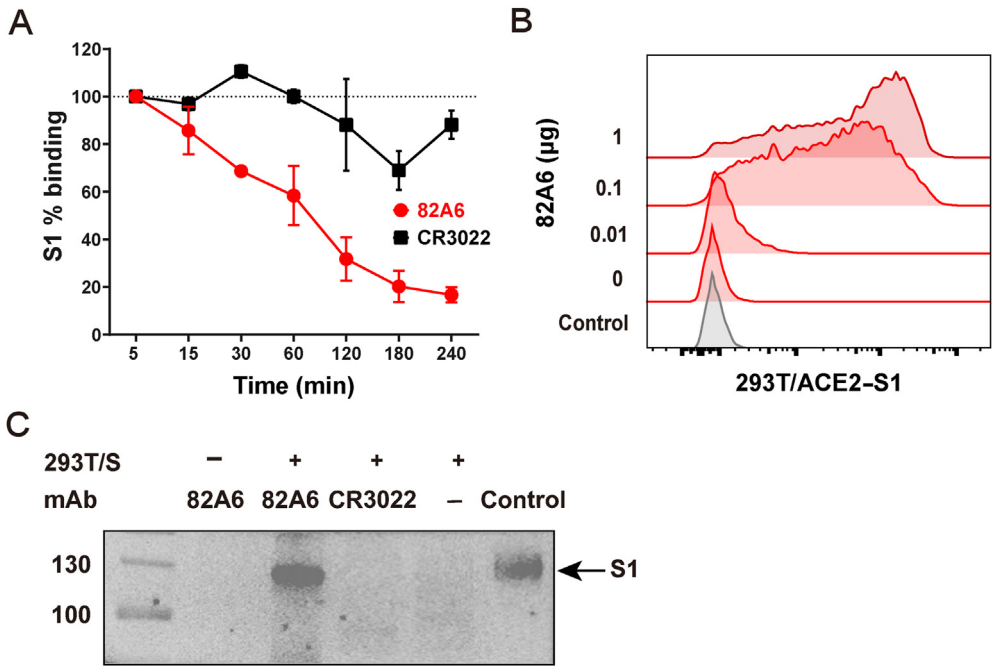

Fig. 3. 82A6 triggered S1 shedding. (A) The binding activity of 82A6 to cell-surface expressed SARS-CoV-2 S protein over time, determined by flow cytometry. CR3022 is included as the negative control (n = 3, presented as mean ± SEM). (B) Flow cytometry analysis for the S1 subunits in the cell supernatant with the incubation of different amount of 82A6. (C) The S1 subunit in the cell supernatant was detected by Western blot analysis. The control was the SARS-CoV-2 Spike S1-His Recombinant Protein (Sino Biological, Beijing, China). Data were obtained from a representative experiment of three replicates.

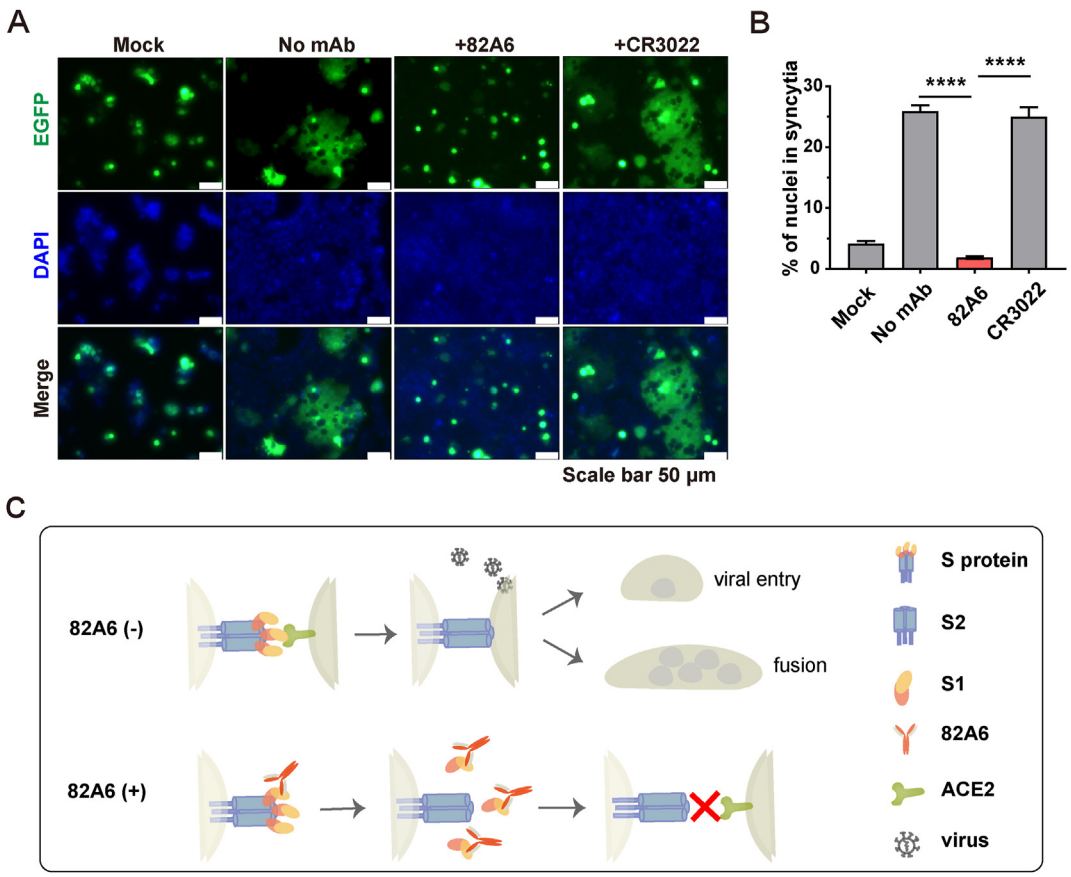

Fig. 4. 82A6 blocked syncytia formation. (A) The fluorescent analysis of syncytia formation. Mock refers to negative control containing only EGFP-labeled 293T/S cells. (B) Quantitative analysis of syncytia in Fig. 4A (n = 3; ****$p < 0.0001$). (C) A schematic illustration for the process of viral entry and syncytia formation (the upper panel), and the neutralizing mechanism of 82A6 (the lower panel).

4. Discussion

In our study, we presented a RBD specific mAb 82A6 that exerted neutralizing efficacy against authentic SARS-CoV-2 virus by inducing S1 shedding. Unlike the majority of RBD-targeted neutralizers, 82A6 was unable to block the RBD-ACE2 interaction which indicated that 82A6 targeted the non-RBM region. This was supported, to a certain extent, by the identification of potential linear antigenic site for 82A6. Further, we confirmed that 82A6 could effectively promote the dissociation of the S1 subunit from the surface-expressed S trimers on 293T/S cells, in both time- and dose-dependent manners. Importantly, 82A6 was capable to effectively abolish the cell fusion between 293T/ACE2 and 293T/S cells, indicating its unique effect in preventing syncytia formation, which was reported signature of COVID-19 severity [23,24]. The identified neutralizing mechanism of 82A6 provided important information for understanding the non-RBM targeted Abs with profound efficacy to block SARS-CoV-2.

To date, most neutralizing Abs reported to induce S1 shedding target the RBM region within RBD [10,18–20]. Because of the high similarity in the epitopes for these RBM-specific Abs, they likely induce comparable RBD conformational change and the consequential S1 dissociation by mimicking the natural receptor [10,18–20]. It is rather surprising for us to find that 82A6, a non-RBM targeted mAb, could induce the same deconstruction of the S protein and release the S1 subunit prior to the binding of ACE2. This may be the result of allosteric recognition, which was shown for another mAb targeting the non-RBM [26]. Given the fact that non-RBM targeted mAbs constituted nearly half of the RBD specific mAbs [28], the identified mechanism of 82A6 may call for attentions to these otherwise overlooked Abs for the neutralization of SARS-CoV-2.

By large, the S1 shedding induced by 82A6 may decrease the availability of intact SARS-CoV-2 virus. There may be other potential advantages of this mAb during the neutralization process. For example, the dissociated 82A6-bound S1 subunits can still bind to ACE2, and keep it “capped”. This may, in one hand, reduce the access of additional viral RBD to its natural receptor; in another hand, prevent the formation of abnormal fusion of cells bearing ACE2 and infected cells expressing viral S protein on the surface. 82A6 exhibit no steric hindrance between RBD and ACE2. This means 82A6 might not be able to stop the recognition of other RBM-targeted neutralizers, if presented, to the free 82A6-S1 complexes. Therefore, efficient clearance of these dissociated complexes needs to be further addressed, which may greatly increase the efficacy of combination treatment using 82A6 and potent RBM specific neutralizers. Nevertheless, the unique role of 82A6 to effectively prevent the formation of multinuclear cells may be informative for optimizing the therapeutic regimen for those COVID-19 patients in advanced stages.

Future work of detailed structure analyses by cryo-electron microscopy (cryo-EM) may help us to understand the precise conformation of RBD in complex with 82A6, as well as the steric epitope recognized by this mAb. Also, the knowledge obtained from such structural study may contribute towards a more comprehensive explanation for the S1 shedding induced by the non-RBM Ab sharing similar neutralizing mechanisms as 82A6.

Taken together, we have provided a non-RBM neutralizing Ab that can induce S1 shedding from the S trimer and block the syncytia formation. This mechanism represents a possible explanation for the non-RBM targeted mAbs exhibiting efficient neutralizing capability against SARS-CoV-2. Our findings may be of particular significance for the development of effective interventions for severe COVID-19 cases.

Author contributions

Conceptualization, A.J. and T.L.; laboratory work, Y.L., S.S., F.L., X.H., C.H. Y.W., S.L. H.Z. and B.Z.; writing-original draft preparation, T.L., Y.L. and SS.; writing-review and editing, Y.L., T.L., W.W. and A.J.

Funding

This work was supported by the Emergency Project from Chongqing Medical University and Chongqing Medical University fund [grant numbers X4457] with the donation from Mr. Yuling Feng.

Institutional review board statement

The project “The application of antibody tests patients infected with SARS-CoV-2” was approved by the ethics committee of Chongqing Medical University.

Declaration of interests

Patent has been filed for some of the antibodies presented here.

Acknowledgments

We acknowledge the clinical laboratories of Yongchuan Hospital of Chongqing Medical University and the Third Affiliated Hospital of Chongqing Medical University for providing blood samples. We are grateful to Wuhan National Biosafety Laboratory and the Key Laboratory of Medical Molecular Virology of Fudan University.

Appendix A. Supplementary data

Supplementary data to this article can be found online at https://doi.org/10.1016/j.bbrc.2021.07.062.

References

[1] K.W. Ng, N. Faulkner, G.H. Cornish, A. Rosa, R. Harvey, S. Hussain, R. Ulferts, C. Earl, et al., Preexisting and de novo humoral immunity to SARS-CoV-2 in humans, Science (New York, N.Y.) 370 (2020) 1339–1343, https://doi.org/10.1126/science.abe1107.

[2] T.J. Ripperger, J.L. Uhrlaub, M. Watanabe, R. Wong, Y. Castaneda, H.A. Pizzato, M.R. Thompson, C. Bradshaw, et al., Orthogonal SARS-CoV-2 serological assays enable surveillance of low-prevalence communities and reveal durable humoral immunity, Immunity 53 (2020) 925–933, https://doi.org/10.1016/j.immuni.2020.10.004, e924.

[3] P. Peng, J. Hu, H.-j. Deng, B.-z. Liu, L. Fang, K. Wang, N. Tang, A.-l. Huang, Changes in the humoral immunity response in SARS-CoV-2 convalescent patients over 8 months, Cell. Mol. Immunol. 18 (2021) 490–491, https://doi.org/10.1038/s41423-020-00605-4.

[4] X. Han, Y. Wang, S. Li, C. Hu, T. Li, C. Gu, K. Wang, M. Shen, et al., A rapid and efficient screening system for neutralizing antibodies and its application for SARS-CoV-2, Front. Immunol. (2021) 12, https://doi.org/10.3389/fimmu.2021.653189.

[5] S. Li, W. Wang, T. Li, X. Han, et al., Immune characteristics analysis reveals two key inflammatory factors correlated to the expressions of SARS-CoV-2 S1-specific antibodies, Gene Dis. (2020), https://doi.org/10.1016/j.gendis.2020.12.007.

[6] J. Lan, J. Ge, J. Yu, S. Shan, H. Zhou, S. Fan, Q. Zhang, X. Shi, et al., Structure of the SARS-CoV-2 spike receptor-binding domain bound to the ACE2 receptor, Nature 581 (2020) 215–220, https://doi.org/10.1038/s41586-020-2180-5.

[7] Q. Wang, Y. Zhang, L. Wu, S. Niu, C. Song, Z. Zhang, G. Lu, C. Qiao, et al., Structural and functional basis of SARS-CoV-2 entry by using human ACE2, Cell 181 (2020) 894–904, https://doi.org/10.1016/j.cell.2020.03.045, e899.

[8] D.J. Benton, A.G. Wrobel, P. Xu, C. Roustan, S.R. Martin, P.B. Rosenthal, J.J. Skehel, S.J. Gamblin, Receptor binding and priming of the spike protein of SARS-CoV-2 for membrane fusion, Nature 588 (2020) 327–330, https://doi.org/10.1038/s41586-020-2772-0.

[9] R. Yan, Y. Zhang, Y. Li, L. Xia, Y. Guo, Q. Zhou, Structural basis for the recognition of SARS-CoV-2 by full-length human ACE2, Science (New York, N.Y.) 367 (2020) 1444–1448, https://doi.org/10.1126/science.abb2762.

[10] J. Ge, R. Wang, B. Ju, Q. Zhang, J. Sun, P. Chen, S. Zhang, Y. Tian, et al., Antibody neutralization of SARS-CoV-2 through ACE2 receptor mimicry, Nat. Commun. 12 (2021) 250, https://doi.org/10.1038/s41467-020-20501-9.
[11] B. Ju, Q. Zhang, J. Ge, R. Wang, J. Sun, X. Ge, J. Yu, S. Shan, et al., Human neutralizing antibodies elicited by SARS-CoV-2 infection, Nature 584 (2020) 115–119, https://doi.org/10.1038/s41586-020-2380-z.
[12] S.J. Zost, P. Gilchuk, J.B. Case, E. Binshtein, R.E. Chen, J.P. Nkolola, A. Schäfer, J.X. Reidy, et al., Potently neutralizing and protective human antibodies against SARS-CoV-2, Nature 584 (2020) 443–449, https://doi.org/10.1038/s41586-020-2548-6.
[13] R. Shi, C. Shan, X. Duan, Z. Chen, P. Liu, J. Song, T. Song, X. Bi, et al., A human neutralizing antibody targets the receptor-binding site of SARS-CoV-2, Nature 584 (2020) 120–124, https://doi.org/10.1038/s41586-020-2381-y.
[14] Y. Wu, F. Wang, C. Shen, W. Peng, D. Li, C. Zhao, Z. Li, S. Li, et al., A noncompeting pair of human neutralizing antibodies block COVID-19 virus binding to its receptor ACE2, Science (New York, N.Y.) 368 (2020) 1274–1278, https://doi.org/10.1126/science.abc2241.
[15] D. Pinto, Y.J. Park, M. Beltramello, A.C. Walls, M.A. Tortorici, S. Bianchi, S. Jaconi, K. Culap, et al., Cross-neutralization of SARS-CoV-2 by a human monoclonal SARS-CoV antibody, Nature 583 (2020) 290–295, https://doi.org/10.1038/s41586-020-2349-y.
[16] C. Wang, W. Li, D. Drabek, N.M.A. Okba, R. van Haperen, A.D.M.E. Osterhaus, F.J.M. van Kuppeveld, B.L. Haagmans, et al., A human monoclonal antibody blocking SARS-CoV-2 infection, Nat. Commun. 11 (2020) 2251, https://doi.org/10.1038/s41467-020-16256-y.
[17] D. Zhou, H.M.E. Duyvesteyn, C.P. Chen, C.G. Huang, T.H. Chen, S.R. Shih, Y.C. Lin, C.Y. Cheng, et al., Structural basis for the neutralization of SARS-CoV-2 by an antibody from a convalescent patient, Nat. Struct. Mol. Biol. 27 (2020) 950–958, https://doi.org/10.1038/s41594-020-0480-y.
[18] N.K. Hurlburt, E. Seydoux, Y.H. Wan, V.V. Edara, A.B. Stuart, J. Feng, M.S. Suthar, A.T. McGuire, et al., Structural basis for potent neutralization of SARS-CoV-2 and role of antibody affinity maturation, Nat. Commun. 11 (2020) 5413, https://doi.org/10.1038/s41467-020-19231-9.
[19] R. Yan, R. Wang, B. Ju, J. Yu, Y. Zhang, N. Liu, J. Wang, Q. Zhang, et al., Structural basis for bivalent binding and inhibition of SARS-CoV-2 infection by human potent neutralizing antibodies, Cell Res. 31 (2021) 517–525, https://doi.org/10.1038/s41422-021-00487-9.
[20] A.Z. Wec, D. Wrapp, A.S. Herbert, D.P. Maurer, D. Haslwanter, M. Sakharkar, R.K. Jangra, M.E. Dieterle, et al., Broad neutralization of SARS-related viruses by human monoclonal antibodies, Science (New York, N.Y.) 369 (2020) 731–736, https://doi.org/10.1126/science.abc7424.
[21] Y. Cai, J. Zhang, T. Xiao, H. Peng, S.M. Sterling, R.M. Walsh Jr., S. Rawson, S. Rits-Volloch, et al., Distinct conformational states of SARS-CoV-2 spike protein, Science (New York, N.Y.) 369 (2020) 1586–1592, https://doi.org/10.1126/science.abd4251.
[22] A.C. Walls, M.A. Tortorici, J. Snijder, X. Xiong, B.J. Bosch, F.A. Rey, D. Veesler, Tectonic conformational changes of a coronavirus spike glycoprotein promote membrane fusion, Proc. Natl. Acad. Sci. U. S. A. 114 (2017) 11157–11162, https://doi.org/10.1073/pnas.1708727114.
[23] R. Bussani, E. Schneider, L. Zentilin, C. Collesi, H. Ali, L. Braga, M.C. Volpe, A. Colliva, et al., Persistence of viral RNA, pneumocyte syncytia and thrombosis are hallmarks of advanced COVID-19 pathology, EBioMedicine 61 (2020) 103104, https://doi.org/10.1016/j.ebiom.2020.103104.
[24] Z. Xu, L. Shi, Y. Wang, J. Zhang, L. Huang, C. Zhang, S. Liu, P. Zhao, et al., Pathological findings of COVID-19 associated with acute respiratory distress syndrome, The Lancet Respiratory Medicine 8 (2020) 420–422, https://doi.org/10.1016/s2213-2600(20)30076-x.
[25] L. Braga, H. Ali, I. Secco, E. Chiavacci, G. Neves, D. Goldhill, R. Penn, J.M. Jimenez-Guardeno, et al., Drugs that inhibit TMEM16 proteins block SARS-CoV-2 spike-induced syncytia, Nature (2021), https://doi.org/10.1038/s41586-021-03491-6.
[26] D. Asarnow, B. Wang, W.-H. Lee, Y. Hu, C.-W. Huang, B. Faust, P.M.L. Ng, E.Z.X. Ngoh, et al., Structural Insight into SARS-CoV-2 Neutralizing Antibodies and Modulation of Syncytia, Cell, 2021, https://doi.org/10.1016/j.cell.2021.04.033.
[27] T. Li, X. Han, C. Gu, H. Guo, H. Zhang, Y. Wang, C. Hu, K. Wang, et al., Ultra-potent SARS-CoV-2 neutralizing antibodies with protective efficacy against newly emerged mutational variants, bioRxiv (2021), https://doi.org/10.1101/2021.04.19.440481, 2021.2004.2019.440481.
[28] W. Dejnirattisai, D. Zhou, H.M. Ginn, H.M.E. Duyvesteyn, P. Supasa, J.B. Case, Y. Zhao, T.S. Walter, et al., The Antigenic Anatomy of SARS-CoV-2 Receptor Binding Domain, Cell, 2021, https://doi.org/10.1016/j.cell.2021.02.032.